AJNR

MR Ventriculography for the Study of CSF Flow

Vivek B. Joseph, Lakshminarayan Raghuram, Ipeson P. Korah and Ari G. Chacko

AJNR Am J Neuroradiol 2003, 24 (3) 373-381
http://www.ajnr.org/content/24/3/373

AJNR Am J Neuroradiol 24:373–381, March 2003

MR Ventriculography for the Study of CSF Flow

Vivek B. Joseph, Lakshminarayan Raghuram, Ipeson P. Korah, and Ari G. Chacko

BACKGROUND AND PURPOSE: **Various MR techniques have been used to assess CSF flow and to image the subarachnoid spaces and ventricles. Anecdotal reports describe the use of intrathecal and intraventricular gadolinium-based contrast agents in humans and animals. We sought to determine the clinical usefulness of gadolinium-enhanced MR ventriculography for assessing CSF flow in patients with various neurologic conditions.**

METHODS: **Five patients (three female and two male patients aged 6 months to 65 years) were included in the study. After performing sagittal, coronal, and axial T1-weighted MR imaging of the brain, 0.02–0.04 mmol of gadodiamide was injected into the lateral ventricle. Sagittal, coronal, and axial T1-weighted imaging was repeated soon after the injection. We were specifically looking for the site of obstruction to CSF flow in those patients with hydrocephalus, communication between cysts and ventricles, elucidation of suspicious intraventricular lesions, and patency of third ventriculostomies.**

RESULTS: **MR ventriculography showed good delineation of the ventricular system in all patients. In one patient with carcinomatosis and hydrocephalus, a block to contrast material flow was detected at the right foramen of Luschka. In another patient with hydrocephalus, partial block to the flow of contrast material was demonstrated at the right foramen of Monro. In a patient with hydrocephalus and a posterior fossa cyst, flow of contrast material was blocked between the third ventricle and the cyst, with a thin streak of contrast material in the aqueduct. As an assessment of the patency of a third ventriculostomy, MR ventriculography showed flow of contrast material into the suprasellar cisterns from the third ventricle in one patient and absence of flow in another.**

CONCLUSION: **MR ventriculography is a safe technique for assessing CSF flow, with application in determining the site of obstruction in hydrocephalus, in assessing communication between cysts and the ventricle, and in determining the functioning status of endoscopic third ventriculostomies.**

Both conventional spin-echo MR imaging and directional flow determination with cine phase-contrast MR imaging have been used to describe flow of CSF in the brain, in a variety of clinical situations (1–10). These studies are noninvasive; however, the spin-echo techniques are less accurate and the cine format when used alone is subjective. The addition of velocity measurements in the phase-contrast technique has improved the accuracy (11, 12). Recently, the 3D constructive interference in steady-state (CISS) sequence has been used for evaluating intraventricular lesions (13). The usefulness of MR imaging with intraventricular or cisternal injections of a gadolinium-based contrast agent to study CSF flow has been reported in animals and humans (14–19). The purpose of our study was to determine the value of MR ventriculography as an adjunct to routine imaging in determining the functional status of third ventriculostomies, in assessing communication between cysts and the ventricles, and in determining the site of CSF block in noncommunicating hydrocephalus.

Methods

We studied five, nonconsecutive patients (three female and two male patients; age range, 6 months to 49 years) with the MR ventriculographic technique between June 2001 and November 2002. All patients and families were explained that this was a new technique with certain risks of central nervous system injury, infection, and contrast material reaction. Permission was obtained from the Fluid Research Grant Committee, Christian Medical College Hospital, Vellore, India, to study the technique. All patients underwent either CT or MR imaging to establish the clinical diagnosis. On the morning of the procedure, an external ventricular drain was inserted into the right frontal horn in the intensive care unit. Subsequently, routine MR imaging was performed and consisted of sagittal, coronal,

Received March 11, 2002; accepted after revision July 31.

From the Departments of Neurological Sciences (V.B.J., A.G.C.) and Radiodiagnosis (L.R., I.P.K.), Christian Medical College Hospital, Vellore, India.

Address reprint requests to Ari G. Chacko, MD, MCh Department of Neurological Sciences, Christian Medical College and Hospital, Vellore 632004, Tamil Nadu, India.

and axial T1-weighted images. Gadodiamide ([1 mL containing 287 mg, 0.5 mmol/mL] Omniscan; Nycomed Ireland Ltd, Cork, Ireland) was diluted (1:50) to a concentration of 0.01 mmol/mL. Two milliliters of CSF was withdrawn by the external ventricular drain, and 2–4 mL of the 1:50 diluted gadodiamide solution (0.02–0.04 mmol) was injected into the ventricle, following which sagittal, coronal, and axial T1-weighted imaging was repeated. The sagittal images were obtained in the prone position for the two patients who had undergone third ventriculostomy. In all patients, the head was gently rotated from side-to-side to allow uniform distribution of the contrast agent. Two patients underwent MR ventriculography while under general anesthesia and were then transported to the operating room while under the same anesthesia for the definitive intracranial procedure.

MR ventriculography was performed with a 0.5-T Gyroscan TS-NT MR imager (Phillips Medical Systems, Best, the Netherlands), with the following parameters: 2D spin-echo sequence was routinely performed with 475/18/1 (TR/TE/NEX), 6-mm section thickness, 0.6-mm section gap, and 90° flip angle.

Results

Patient 1 was a 65-year-old woman who presented with headache and lethargy of 2 months' duration. She had neck stiffness. Contrast material–enhanced CT of the brain showed right frontal and left cerebellar contrast-enhancing tumors with ventriculomegaly (Fig 1A–C). The differential diagnosis was tuberculoma or metastatic tumor. The locations of the tumors did not explain the presence of the hydrocephalus, which included dilatation of the lateral, third, and fourth ventricles. Therefore, the possibility of a carcinomatous meningitis or meningitis due to tuberculosis was considered as a cause of the hydrocephalus. Her sensorium, which continued to deteriorate after admission, improved with external ventricular drainage. To ascertain whether this was a communicating or noncommunicating hydrocephalus, MR ventriculography was performed. The MR ventriculogram demonstrated free communication among the lateral, third, and fourth ventricles (Fig 1D–F). However, while contrast material exited the fourth ventricle via the left foramen of Luschka and foramen of Magendie, no contrast material could be seen in the right foramen of Luschka (Fig 1G and F). The next day, a CT-guided stereotactic biopsy was performed of the right frontal mass, and the findings were reported as metastatic adenocarcinoma. Carcinomatous meningitis was concluded to be the cause of the basal arachnoiditis, and the external ventricular drain was converted to a ventriculoperitoneal shunt. The patient was advised to undergo radiation therapy.

Patient 2 was a 9-year-old girl who presented with headache, vomiting, and two episodes of decerebration of 1 week's duration. She had papilledema with no lateralizing neurologic deficits. The CT scan of the brain showed dilatation of all ventricles (Fig 2A). A suspicious lesion was noted in the fourth ventricle, raising the possibility of a fourth ventricular cysticercus cyst causing the hydrocephalus (Fig 2B). The sagittal MR ventriculogram showed evidence of a syrinx in the cervical and thoracic cord with no tonsillar herniation (Fig 2E). At MR ventriculography, contrast material injected into the right frontal horn demonstrated a partial block to the flow of CSF at the right foramen of Monro despite turning the head 90° to the left to present the contrast material to that region (Fig 2C–E). To determine if the left foramen of Monro was patent, we inserted a left frontal ventricular catheter and injected 4 mL of contrast material into the left frontal horn. The time gap between the studies was 100 minutes. The repeat MR ventriculography showed good flow of contrast material from the left lateral ventricle through the foramen of Monro into the third ventricle. Contrast material from the first injection into the right frontal horn was now more uniformly distributed (Fig 2F–H). It is possible that the layered contrast material in the right lateral ventricle had now diffused more uniformly or that contrast material injected into the left frontal horn refluxed up into the right frontal horn from the third ventricle. There was no obvious lesion within the fourth ventricle. No contrast material was seen exiting the fourth ventricle, and no communication was noted between the fourth ventricle and the cervical syrinx. The patient was taken to the operation room, and a left frontal burr hole was placed. Third ventriculostomy was performed after negotiating the endoscope through the patent left foramen of Monro. In addition, fenestration of the septum pellucidum was performed to establish communication between the lateral ventricles, thus providing drainage for the right lateral ventricle.

The third patient was a 6-month-old girl who presented with an enlarging head since birth. The CT scan of the brain showed hypoplasia of the vermis with a large posterior fossa cyst. There was dilatation of the third and lateral ventricles. MR ventriculography (Fig 3) demonstrated intense contrast in the left lateral ventricle and third ventricle, with contrast of less intensity in the right lateral ventricle (Fig A–C). A thin trickle of contrast material was seen entering the cerebral aqueduct, indicating an aqueductal narrowing (Fig 3A and D). Therefore, shunt tubes were placed in the posterior fossa cyst and in the lateral ventricle (ventriculocystoperitoneal shunt). In this case of a Dandy-Walker malformation, MR ventriculography clearly demonstrated that there was an associated aqueductal stenosis; this information helped in the surgical decision-making process.

Patient 4 was an 8-year-old boy who presented with headache and vomiting of 3 months' duration. He had bilateral papilledema, sixth nerve palsies, and cerebellar signs. A CT scan of the brain showed an enhancing midline posterior fossa mass causing hydrocephalus. Since he was symptomatic and time was not available on the elective operating list for removal of the posterior fossa mass, an endoscopic third ventriculostomy was performed. Although he had complete relief of raised intracranial symptoms, a subgaleal collection of CSF at the burr-hole site after 5 days prompted us to ascertain patency of the third ventriculostomy. He was scheduled for posterior fossa surgery the next day, and MR ventriculography was planned while the patient was under the general anesthesia for surgery. MR ventriculography demon-

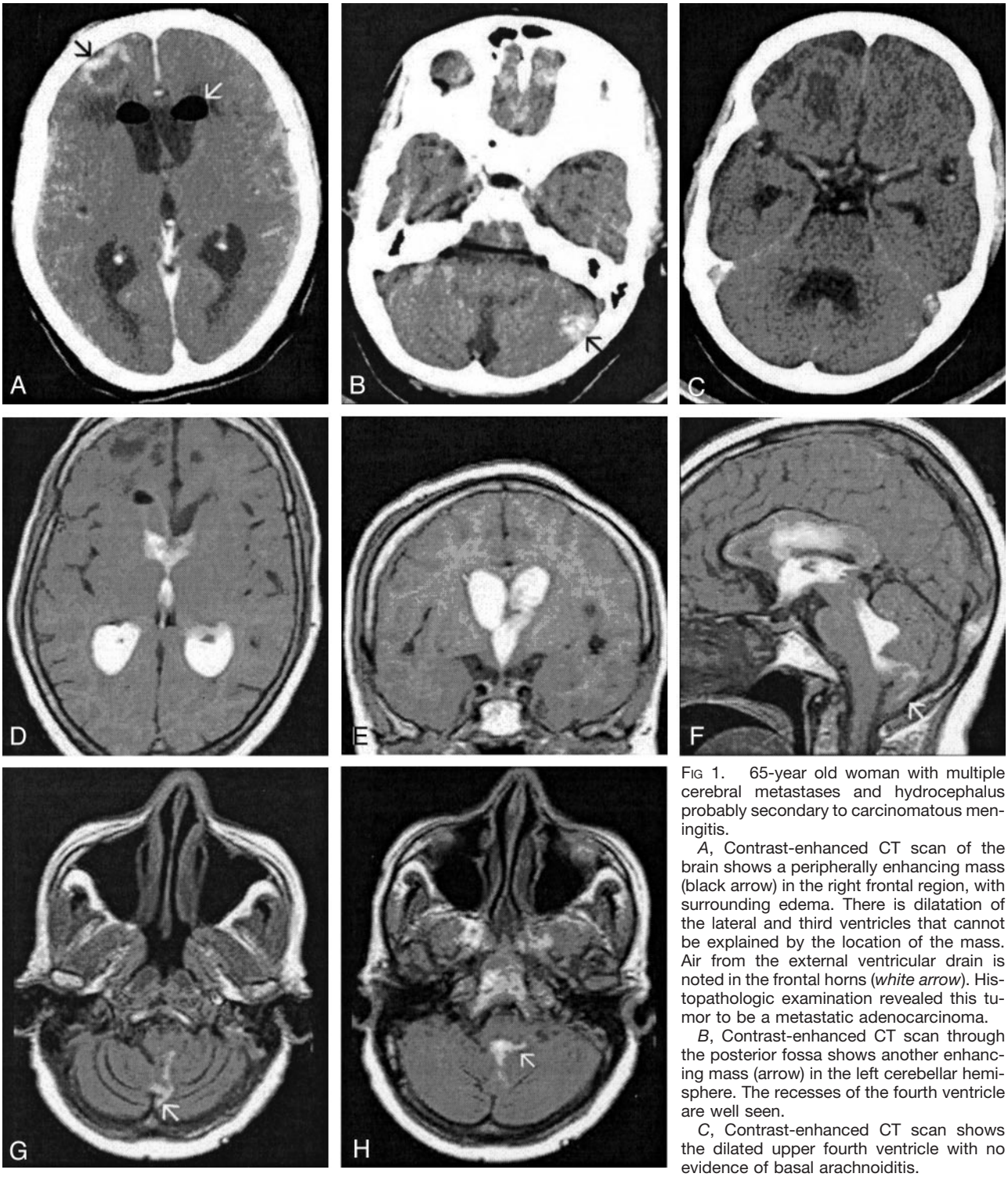

FIG 1. 65-year old woman with multiple cerebral metastases and hydrocephalus probably secondary to carcinomatous meningitis.

A, Contrast-enhanced CT scan of the brain shows a peripherally enhancing mass (black arrow) in the right frontal region, with surrounding edema. There is dilatation of the lateral and third ventricles that cannot be explained by the location of the mass. Air from the external ventricular drain is noted in the frontal horns (*white arrow*). Histopathologic examination revealed this tumor to be a metastatic adenocarcinoma.

B, Contrast-enhanced CT scan through the posterior fossa shows another enhancing mass (arrow) in the left cerebellar hemisphere. The recesses of the fourth ventricle are well seen.

C, Contrast-enhanced CT scan shows the dilated upper fourth ventricle with no evidence of basal arachnoiditis.

D, Axial MR ventriculogram shows contrast material in the lateral and third ventricles.

E, Coronal MR ventriculogram shows contrast material in both lateral ventricles, open foramina of Monro, and third ventricle. There is no contrast material in the basal subarachnoid cisterns.

F, Sagittal MR ventriculogram shows contrast material in the lateral, third, and fourth ventricles. Note contrast material exiting the fourth ventricle through the foramen of Magendie into the cisterna magna (*arrow*).

G, Axial MR ventriculogram shows contrast material in the lower fourth ventricle exiting the foramen of Magendie. Note the absence of contrast material in the right foramen of Luschka.

H, Axial MR ventriculogram shows contrast material in the lower fourth ventricle entering the left foramen of Luschka (*white arrow*). Note the absence of contrast material in the right foramen of Luschka. The absence of contrast material in the basal subarachnoid spaces and the block in the right foramen of Luschka led us to a diagnosis of basal arachnoiditis due to leptomeningeal seeding in this patient with metastatic adenocarcinoma.

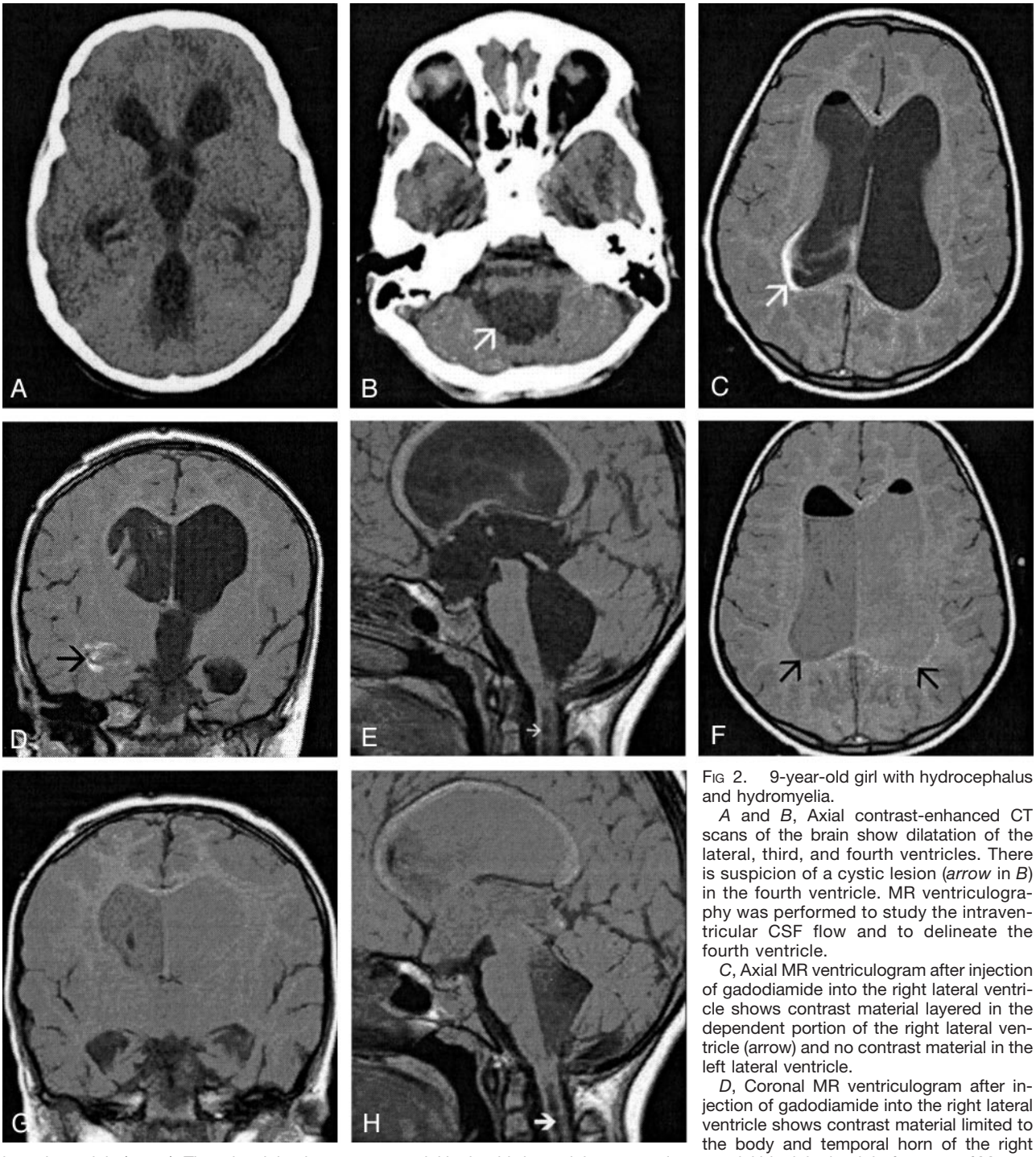

FIG 2. 9-year-old girl with hydrocephalus and hydromyelia.

A and *B*, Axial contrast-enhanced CT scans of the brain show dilatation of the lateral, third, and fourth ventricles. There is suspicion of a cystic lesion (*arrow* in *B*) in the fourth ventricle. MR ventriculography was performed to study the intraventricular CSF flow and to delineate the fourth ventricle.

C, Axial MR ventriculogram after injection of gadodiamide into the right lateral ventricle shows contrast material layered in the dependent portion of the right lateral ventricle (arrow) and no contrast material in the left lateral ventricle.

D, Coronal MR ventriculogram after injection of gadodiamide into the right lateral ventricle shows contrast material limited to the body and temporal horn of the right lateral ventricle (*arrow*). There is minimal contrast material in the third ventricle, suggesting a partial block in the right foramen of Monro.

E, Sagittal MR ventriculogram after injection of contrast material into the right lateral ventricle shows minimal contrast material entering the third and fourth ventricles. Note the presence of a syringomyelia in the upper cervical cord (*arrow*).

F, Axial MR ventriculogram through the bodies of the lateral ventricles. Contrast material was injected into the left lateral ventricle 100 minutes after the previous injection into the right lateral ventricle. This image shows a more uniform distribution of the contrast material in the right lateral ventricle, with no evidence of layering.

G, Coronal MR ventriculogram after injection of contrast material into the left lateral ventricle shows good flow of the contrast material through the left foramen of Monro into the third ventricle.

H, Sagittal MR ventriculogram shows flow of contrast material from the third ventricle into the fourth ventricle with no intraventricular lesion. The syrinx in the upper cervical cord (arrow) is again noted.

strated that the third ventriculostomy was not functioning (Fig 4). The patient was taken directly to the operation room. Intraoperatively, the tumor had not infiltrated the floor of the fourth ventricle, and after radical excision, the cerebral aqueduct was completely open with free flow of CSF. The biopsy find-

FIG 3. 6-month-old girl with a Dandy-Walker malformation and aqueductal stenosis.

A, Sagittal MR ventriculogram shows intense contrast in the left lateral and third ventricles. The anterior recesses of the third ventricle (*white arrow*) and the massa intermedia (*black arrow*) are clearly visible. There is a thin trickle of contrast material in the cerebral aqueduct, indicating a relative stenosis. The asterisk (*) indicates the posterior fossa cyst.

B, Coronal MR ventriculogram shows intense contrast in the body of the left lateral ventricle, third ventricle, and the left temporal horn. Contrast in the right lateral ventricle is of less intensity (*X*).

C, Axial MR ventriculogram shows contrast in the third ventricle (*arrow*) and the left temporal horn (*arrowhead*). Contrast of less intensity fills the right temporal horn. The posterior fossa cyst (*) has no contrast.

D, Axial MR ventriculogram shows intense contrast in the anteroinferior part of the third ventricle (white arrow) and temporal horn of the left lateral ventricle, and a thin trickle of contrast material in the cerebral aqueduct (*black arrow*) entering the posterior fossa cyst (*)

ings were reported as medulloblastoma. The postoperative contrast-enhanced CT scan (Fig 4F) showed no residual tumor. He was given a course of postoperative craniospinal radiation therapy.

The fifth patient was a 49-year-old man who presented with headache and neck pain for 3 months' duration. There was papilledema, bilateral sixth nerve palsies, and cerebellar signs with no lower cranial nerve palsies. MR imaging showed a midline cyst in the posterior fossa with a solid, enhancing component at C1–2, causing hydrocephalus. After third ventriculostomy, symptoms of raised intracranial pressure were relieved. MR ventriculography performed 6 days later (Fig 5) demonstrated a functioning third ventriculostomy. He underwent total excision of the mass, which was reported to be a cystic neurofibroma at histopathologic examination.

Discussion

Special radiologic studies are required to assess relative or absolute obstruction to CSF flow in various clinical conditions. Assessing communication between cysts and the ventricular system, patency of third ventriculostomies, and the site of obstruction in obstructive hydrocephalus, as well as detection of intraventricular cysticerci has relevance in directing appropriate therapy. Although conventional x-ray ventriculography (20), metrizamide CT ventriculography or cisternography, and isotope cisternography (21) are relatively inexpensive, their poor spatial resolution, lack of multiplanar imaging capability, and exposure to radiation are drawbacks.

With the introduction of MR imaging, newer techniques for assessing flow without these disadvantages were possible. These included CSF flow studies by using spin-echo sequences, cine phase-contrast MR imaging for directional flow determination, and the 3D Fourier transform sequence, CISS (1–8, 10–12, 21–23). Jack and Kelly (6), in an assessment of third ventriculostomy patency, described a CSF flow void in the floor of the third ventricle on T2-weighted images. Although this could signify rapid, turbulent flow through a perforation, the presence of the basilar artery in the vicinity of the expected third ventriculostomy flow void made interpretation difficult, with false-positive results. Moreover, they found that the absence of a flow void did not preclude adequate function, as the use of flow-compensation techniques may have yielded the false-negative results.

Subsequently, cine 2D phase-contrast MR imaging methods were used to assess CSF flow and patency of third ventriculostomies. Lev et al (3) used a cine phase-contrast MR imaging technique to measure

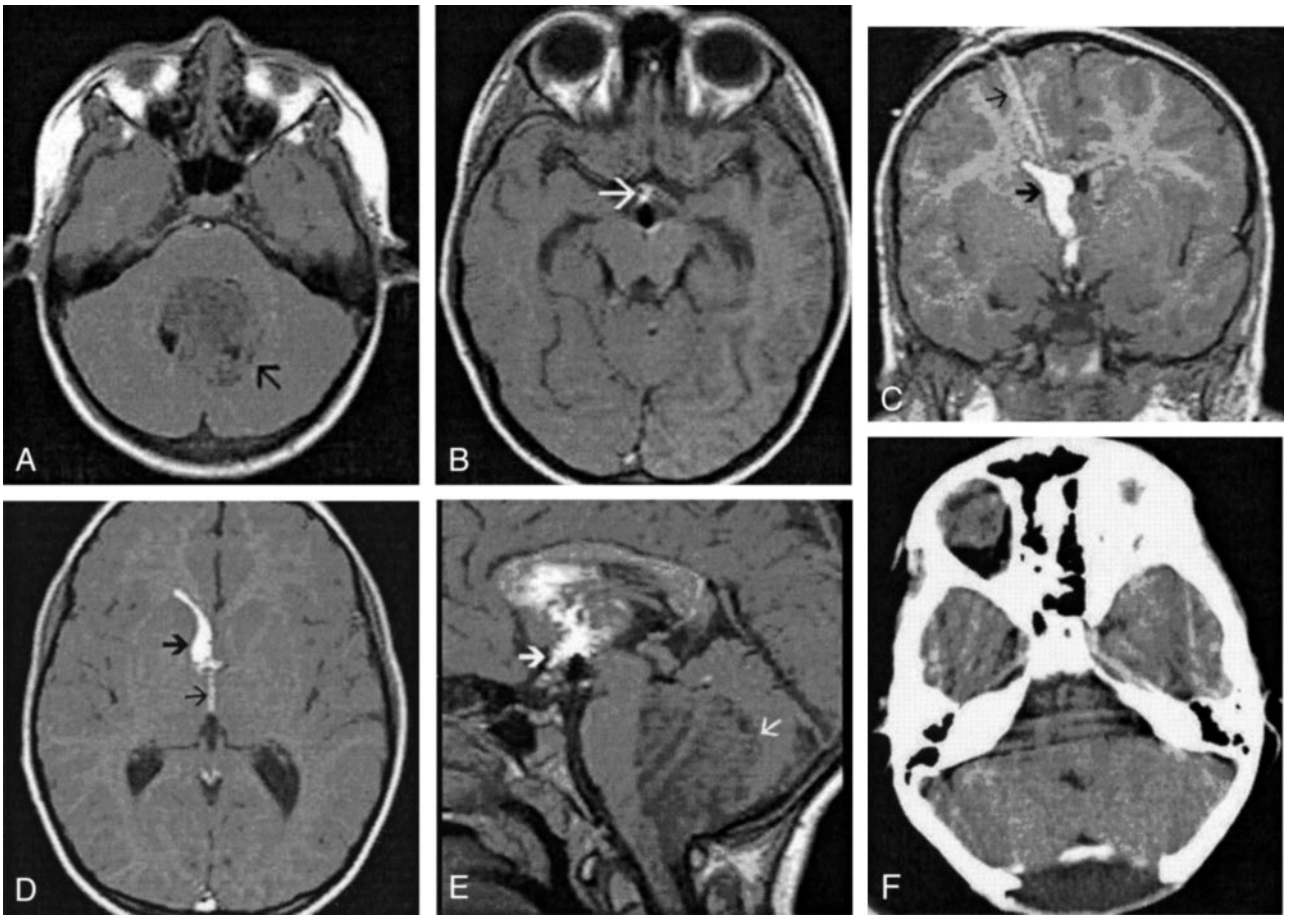

FIG 4. 8-year-old boy with a medulloblastoma and hydrocephalus who underwent an emergency third ventriculostomy before excision of the tumor.

A, Nonenhanced axial T1-weighted MR image shows a large hypointense tumor (*arrow*) in the posterior fossa.

B, Axial MR ventriculogram after third ventriculostomy shows contrast material in the anteroinferior third ventricle (*arrow*). Note that there is no contrast material in the adjacent suprasellar and sylvian cisterns.

C, Coronal ventriculogram after third ventriculostomy shows contrast material along the external ventricular drain (*thin arrow*), the frontal horn of the right lateral ventricle (*thick arrow*), and the third ventricle. Note that no contrast material is seen in the suprasellar cisterns.

D, Axial MR ventriculogram after third ventriculostomy shows contrast material in the right frontal horn (*thick arrow*) and third ventricle (*thin arrow*).

E, Sagittal MR ventriculogram after third ventriculostomy shows contrast material in the dependent portion of the lateral ventricle and the third ventricle (*thick arrow*). There is no contrast material seen in suprasellar cisterns. Note the large hypointense tumor (*thin arrow*) in the posterior fossa.

F, Postoperative contrast-enhanced CT scan through the posterior fossa shows complete tumor excision.

actual flow velocities and velocity ratios between the third ventricular floor and cervical subarachnoid space in six patients with third ventriculostomies and 12 control subjects. They found higher velocities at the third ventricular floor and prepontine cistern in the patients compared with velocities in the control subjects, indicating a patent ventriculostomy. However, even in the control subjects, flow was detectable in the floor of the third ventricle. Therefore, modest flow in the region is inconsequential and does not indicate patency of the third ventriculostomy. This was corroborated by Fukuhara et al (8) who compared cine phase-contrast MR imaging and direct endoscopic exploration of the third ventriculostomy orifice in 12 patients. In five patients with no flow on phase-contrast MR images, the ventriculostomies were closed with a membrane or clot. However, in four patients in whom flow was considered "subtle" before exploration, all had membranes across the orifice, requiring fenestration.

Compared with the standard MR images, a 3D Fourier transform sequence—CISS—produces greater detail of the ventricular system and basal cisterns, with excellent CSF-to-brain contrast and superior spatial resolution (22, 23). Moreover, this technique may define cyst walls and septations better since the adjacent flow patterns can enhance the visualization of these septations. Govindappa et al (13) found CISS more sensitive and specific than routine spin-echo sequences in the diagnosis of intraventricular cysticercal cysts. Aleman et al (23) used the CISS technique with T2-weighted imaging before and after fenestration procedures for loculated or multiloculated hydrocephalus, aqueductal stenosis or obstruction, and

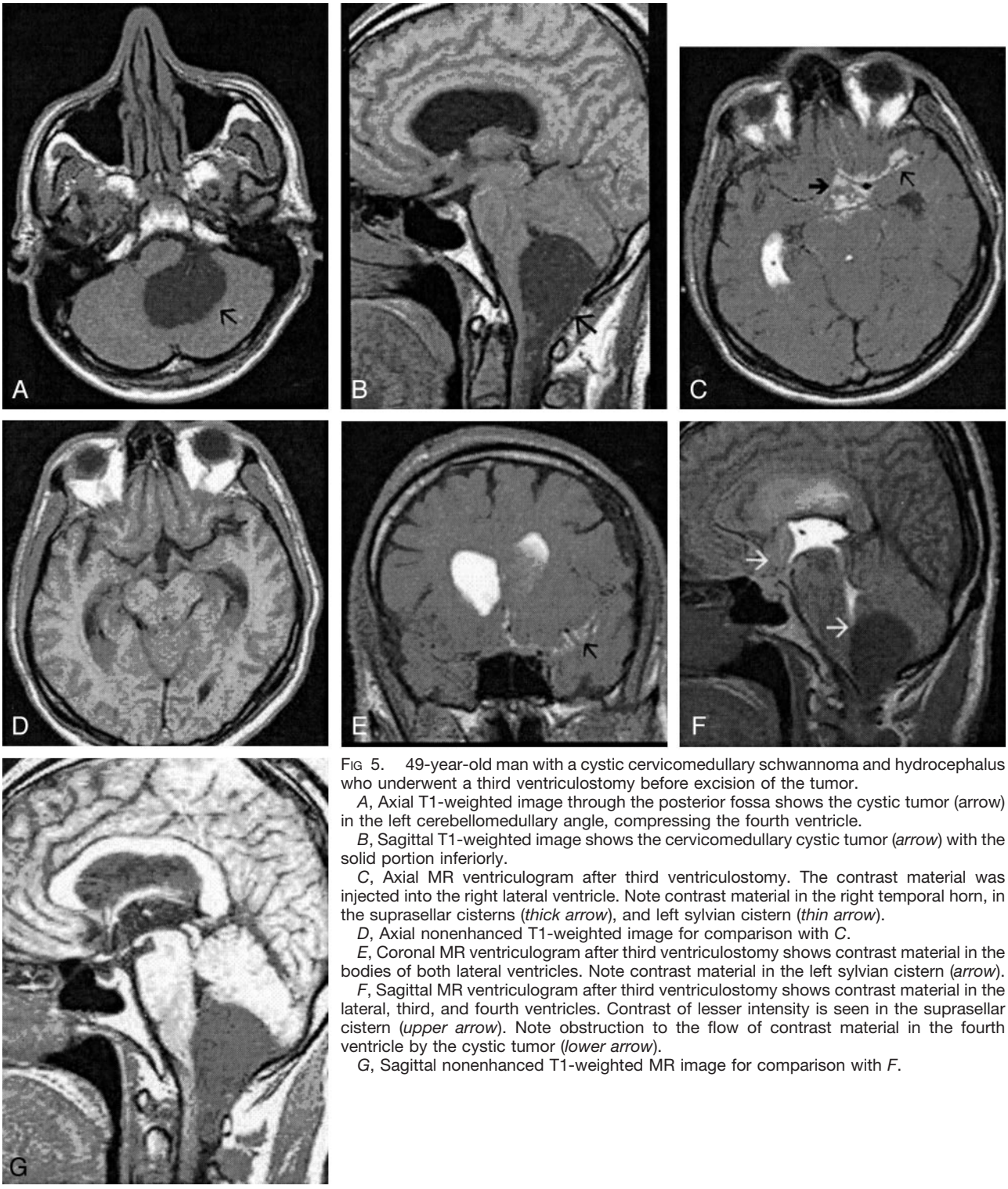

FIG 5. 49-year-old man with a cystic cervicomedullary schwannoma and hydrocephalus who underwent a third ventriculostomy before excision of the tumor.

A, Axial T1-weighted image through the posterior fossa shows the cystic tumor (arrow) in the left cerebellomedullary angle, compressing the fourth ventricle.

B, Sagittal T1-weighted image shows the cervicomedullary cystic tumor (*arrow*) with the solid portion inferiorly.

C, Axial MR ventriculogram after third ventriculostomy. The contrast material was injected into the right lateral ventricle. Note contrast material in the right temporal horn, in the suprasellar cisterns (*thick arrow*), and left sylvian cistern (*thin arrow*).

D, Axial nonenhanced T1-weighted image for comparison with *C*.

E, Coronal MR ventriculogram after third ventriculostomy shows contrast material in the bodies of both lateral ventricles. Note contrast material in the left sylvian cistern (*arrow*).

F, Sagittal MR ventriculogram after third ventriculostomy shows contrast material in the lateral, third, and fourth ventricles. Contrast of lesser intensity is seen in the suprasellar cistern (*upper arrow*). Note obstruction to the flow of contrast material in the fourth ventricle by the cystic tumor (*lower arrow*).

G, Sagittal nonenhanced T1-weighted MR image for comparison with *F*.

intracranial cysts by using a flexible endoscope in 14 consecutive patients. The preoperative CISS images demonstrated intracystic and intraventricular septa not observed with conventional T2-weighted imaging in 11 of 15 procedures. Both CISS and T2-weighted imaging demonstrated flow voids through third ventriculostomies. Although CISS could clearly demonstrate the fenestration performed for six of nine intracranial cysts, no flow void through the fenestration was observed. This was possibly because the pressure gradient between cysts and ventricle was too small to produce a high CSF flow and flow voids.

The use of slow-flow pulse sequences based on a 3D steady-state free precession (SSFP) scheme with additional gradient pulses in the read-out axis provides a very high sensitivity to fluid motion, down to flow velocities of 0.5–1.0 mm/s in phantom studies (24). This sequence has provided valuable informa-

tion on CSF flow in head and spine disorders (24, 25). In the assessment of spinal stenosis, the slow-flow sequence detected a distinct flow pattern in high-grade stenoses; however, in intermediate- and low-grade stenoses, it was less reliable (25). These flow sensitive and diffusion-weighted MR imaging sequences were useful in the study of clinically suspected CSF leaks (26). In the evaluation of 24 sacral meningeal cysts, Davis et al (24) found that flow sensitive MR imaging was useful in detecting communication between the cysts and the subarachnoid space in those patients who were symptomatic, whereas the asymptomatic cysts were noncommunicating. The CISS technique is not readily available and is dependent on a correct gradient strength.

The technique of MR ventriculography involves the acquisition of T1-weighted sequences after injection of a gadolinium-based contrast agent into the ventricles (MR ventriculography) or into the lumbar subarachnoid space (MR cisternography). There have been a few reports showing that the technique is safe and provides accurate information regarding obstruction to CSF flow (14–19). In studies on rats by Ray et al (17, 18), gadopentetate dimeglumine and gadodiamide or caldiamide at low doses adequate for imaging purposes, caused no histologic or behavioral changes. In another study by Skalpe and Tang (19), who used these two preparations of gadolinium-based contrast agents in eight pigs, marked enhancement of the CSF was obtained with concentrations from 10 to 0.625 mmol/L. They concluded that both these gadolinium-based compounds were remarkably well tolerated in the subarachnoid space and in doses relevant for imaging purposes; no adverse effects were seen. Siebner et al (14) reported on two cases of leptomeningeal carcinomatosis studied with MR ventriculography with use of 0.01 mmol of gadopentetate dimeglumine. They found excellent contrast between ventricular CSF and brain and a high safety index. Zeng et al (16) performed MR cisternography with intrathecal lumbar injection of gadopentetate dimeglumine at doses ranging from 0.1 to 0.5 mmol in 11 patients. No complications were noticed in any of the 11 patients during a 9–15 month follow-up. The imaging was helpful in identifying disk herniation, posttraumatic spinal stenosis, postsurgical noncommunicating cyst, myelitis, intradural extramedullary mass, and vascular malformation.

In our report of five patients, we evaluated the usefulness of MR ventriculography in an assortment of clinical situations. MR ventriculography showed unequivocal block at the foramen of Luschka in the first patient, evidence of patency of third ventriculostomy in the fourth patient, and a nonfunctioning ventriculostomy in the fifth patient. It also showed a lack of communication between dilated ventricles and a posterior fossa cyst in the third patient and partial obstruction at the right foramen of Monroe in the second patient. In these latter two patients, the surgical procedures performed were based on the imaging findings. The administration of intraventricular contrast material in such low doses (0.02–0.04 mmol giving a dose of 0.01–0.02 mmol/g of brain) appears to be safe, and no complications occurred after its use in our study.

The primary advantage of MR flow studies and flow sensitive sequences over MR ventriculography is related to the potential for repeated imaging for follow-up studies since they are noninvasive. MR ventriculography, being invasive, would primarily find its use for diagnostic purposes, aiding in clinical decision making. In the case of intermittent obstructions to flow, assessment of ventricular or cyst wall compliance and the possible detection of one-way or bidirectional flow, SSFP studies would be advantageous.

CT cisternography has been shown to predict surgical outcome in patients with normal-pressure hydrocephalus; patients with persistent ventricular stasis had an unsatisfactory response to shunt surgery (27). Radionuclide CSF flow studies have been used in assessing CSF flow patterns in the spinal and cranial subarachnoid spaces. These findings were used to predict homogeneous distribution of intrathecal chemotherapy for patients with leptomeningeal metastasis (28). Unlike CT cisternography, MR ventriculography and MR cisternography do not have the problems related to radiation. Although radionuclide cisternography imparts a lower radiation exposure, it may involve a longer duration of examination. MR cisternography would therefore be a superior technique in the evaluation of ventricular stasis and in documenting CSF flow patterns for homogeneous distribution of intrathecal chemotherapy. Furthermore, with MR ventriculography, there is better delineation of adjacent soft-tissue characteristics, and it is possible to perform additional physiologic studies, such as cerebral blood flow and diffusion. Other applications of MR ventriculography and MR cisternography may include evaluation of CSF flow across the craniospinal junction in syringomyelia. In the evaluation of CSF dural fistulas, T2-weighted MR images have been found to be more sensitive than CT cisternography and radionuclide cisternography (25). The latter techniques deliver a high dose of radiation, are cumbersome and invasive, and in the absence of an active leak may have high false-negative rates. However, CT defines bone very well and would be a useful additional tool to detect bone defects in CSF dural fistulas and to describe bone anomalies at the craniovertebral junction. Further studies may indicate a role for MR cisternography in defining with greater detail the CSF pathways in relation to adjacent soft tissues, thus enabling detection of CSF dural fistulas.

Conclusion

Apart from the noninvasive MR flow studies available, MR ventriculography is a safe additional technique that may be used to ascertain patency of third ventriculostomies. It is likely to help in differentiating between intracranial cysts and enlargement of CSF spaces and in the assessment of intraventricular masses. MR cisternography can provide excellent detail of the contrast material pathways in relation to

adjacent soft tissues and the ventricular system. Both MR ventriculography and MR cisternography maybe used in the setting of a routine MR imaging examination including T1-weighted, T2-weighted, diffusion, perfusion, and contrast-enhanced studies. We foresee the greater use of MR ventriculography or MR cisternography in understanding CSF flow dynamics in physiologic and pathologic states.

References

1. Wolpert SM, Bhadelia RA, Bogdan AR, Cohen AR. **Chiari I malformations: assessment with phase-contrast velocity MR.** *AJNR Am J Neuroradiol* 1994;15:1299–1308
2. Enzmann DR, Pelc NJ. **Normal flow patterns of intracranial and spinal cerebrospinal fluid defined with phase-contrast cine MR imaging.** *Radiology* 1991;178:467–474
3. Lev S, Bhadelia RA, Estin D, Heilman CB, Wolpert SM. **Functional analysis of third ventriculostomy patency with phase-contrast MRI velocity measurements.** *Neuroradiology* 1997;39:175–179
4. Quencer RM. **Intracranial CSF flow in pediatric hydrocephalus: evaluation with cine-MR imaging.** *AJNR Am J Neuroradiol* 1992; 13:601–608
5. Mascalchi M, Arnetoli G, Inzitari D, et al. **Cine-MR imaging of aqueductal CSF flow in normal pressure hydrocephalus syndrome before and after CSF shunt.** *Acta Radiol* 1993;34:586–592
6. Jack CR Jr, Kelly PJ. **Stereotactic third ventriculostomy: assessment of patency with MR imaging.** *AJNR Am J Neuroradiol* 1989; 10:515–522
7. Hoffman KT, Hosten N, Meyer BU, et al. **CSF flow studies of intracranial cysts and cyst-like lesions achieved using reversed fast imaging with steady-state precession MR sequences.** *AJNR Am J Neuroradiol* 2000;21:493–502
8. Fukuhara T, Vorster SJ, Ruggieri P, Luciano MG. **Third ventriculostomy patency: comparison of findings at cine phase-contrast MR imaging and at direct exploration.** *AJNR Am J Neuroradiol* 1999;20:1560–1566
9. Parkkola RK, Komu ME, Aarimaa TM, Alanen MS, Thomsen C. **Cerebrospinal fluid flow in children with normal and dilated ventricles studied by MR Imaging.** *Acta Radiol* 2001;42:33–38
10. Ernst S, Ernestus RI, Kugel H, Lackner K. **MRI with cerebrospinal fluid measurement before and after endoscopic ventriculostomy and aqueductal stenosis.** *Rofo Fortschr Geb Rontgestr Neuen Bildgeb Verfahr* 2001;173:502–508
11. Bhadelia RA, Bogdan AR, Wolpert SM, Lev S, Appignani BA, Hellman CB. **Cerebrospinal fluid flow waveforms: analysis in patients with Chiari I malformation by means of gated phase-contrast MR imaging velocity measurements.** *Radiology* 1995;196:195–202
12. Bhadelia RA, Bogdan AR, Wolpert SM. **Analysis of cerebrospinal fluid flow waveforms with gated phase-contrast MR velocity measurements.** *AJNR Am J Neuroradiol* 1995;16:389–400
13. Govindappa SS, Narayanan JP, Krishnamoorthy VM, Shastry CH, Balasubramaniam A, Krishna SS. **Improved detection of intraventricular cysticercal cysts with the use of three-dimensional constructive interference in steady state MR sequences.** *AJNR Am J Neuroradiol* 2000;21:679–684
14. Siebner HR, Grafin von Einsiedel H, Conrad B. **Magnetic resonance ventriculography with gadolinium DTPA: report of two cases.** *Neuroradiology* 1997;39:418–422
15. Toney GM, Chavez HA, Ibara R, Jinkins JR. **Acute and subacute physiological and histological studies of the central nervous system after intrathecal gadolinium injection in the anesthetized rat.** *Invest Radiol* 2001;36:33–40
16. Zeng Q, Xiong L, Jinkins JR, Fan Z, Liu Z. **Intrathecal gadolinium-enhanced MR myelography and cisternography: a pilot study in human patients.** *AJR Am J Roentgenol* 1999;173:1109–1115
17. Ray DE, Holton JL, Nolan CC, Cavanagh JB, Harpur ES. **Neurotoxic potential of gadodiamide after injection into the lateral cerebral ventricle of rats.** *Am J Neuroradiol* 1998;19:1455–1462
18. Ray DE, Cavanagh JB, Nolan CC, Williams SCR. **Neurotoxic effects of gadopentetate dimeglumine: behavioural disturbance and morphology after intracerebroventricular injection in rats.** *Am J Neuroradiol* 1996;17:365–373
19. Skalpe IO, Tang GJ. **Magnetic resonance imaging contrast media in the subarachnoid space: a comparison between gadodiamide injection and gadopentetate dimeglumine in an experimental study in pigs.** *Invest Radiol* 1997;32:140–148
20. Taveras JM, Wood EH. **Pneumoencephalography**. In: Taveras JM, Wood EH, eds. *Diagnostic Neuroradiology.* 2nd ed. Baltimore: Williams and Wilkins, 1976:232–233
21. Stevens JM, Murray AD, Saunders D, Lane B. **Cranial and intracranial pathology.** In: Grainger RG, Allison DJ, Adam A, Dixon AK, eds. *Grainger & Allison's Diagnostic Radiology—A Textbook of Medical Imaging.* 4th ed. London: Churchill Livingstone, Harcourt Publishers Limited, 2001:2404
22. Laitt RD, Malluci CL, Jaspan T, McConachie NS, Vloeberghs M, Punt J. **Constructive interference in steady-state 3D Fourier-transform MRI in management of hydrocephalus and third ventriculostomy.** *Neuroradiology* 1999;41:117–123
23. Aleman J, Jokura H, Higano S, Akabane A, Shirane R, Yoshimoto T. **Value of constructive interference in steady-state, three-dimensional, Fourier transformation magnetic resonance imaging for the neuroendoscopic treatment of hydrocephalus and intracranial cysts.** *Neurosurgery* 2001;48:1291–1296
24. Davis SW, Levy LM, LeBihan DJ, Rajan S, Schellinger D. **Sacral meningeal cysts: evaluation with MR imaging.** *Radiology* 1993;187: 445–448
25. Schellinger D, LeBihan D, Rajan SS, et al. **MR of slow CSF flow in the spine.** *AJNR Am J Neuroradiol* 1992;13:1393–1403
26. Levy LM, Gulya AJ, Davis SW, LeBihan D, Rajan SS, Schellinger D. **Flow-sensitive magnetic resonance imaging in the evaluation of cerebrospinal fluid leaks.** *Am J Otol* 1995;16:591–596
27. Chang CC, Kuwana N, Ito S, Ikegami T. **Prediction of effectiveness of shunting in patients with normal pressure hydrocephalus by cerebral blood flow measurement and computed tomography cisternography.** *Neurol Med Chir (Tokyo)* 1999;39:841–846
28. Chamberlain MC. **Radioisotope CSF flow studies in leptomeningeal metastases.** *J Neurooncol* 1998;38:135–140